DESIGN AND FABRICATION OF AUTOMATIC TILT ANGLE ADJUSTMENT DEVICE FOR PRECISION MEASUREMENT APPLICATION

Tran Minh Sang*, Luu Duc Binh, Do Le Hung Toan, Tran Minh Thong, Pham Nguyen Quoc Huy, Vo Nhu Thanh

The University of Danang – University of Science and Technology, Vietnam

*Corresponding author: tmsang@dut.udn.vn

(Received: July 22, 2024; Revised: August 26, 2024; Accepted: September 06, 2024)

DOI: 10.31130/ud-jst.2024.338E

Abstract - This article describes the design and fabrication of an angle tilt adjustment device that automatically adjusts the measured surface to parallel the surface plate. The device features a 150 mm × 150 mm worktable and enables independent tilt adjustment of the worktable surface in the X and Y directions via two worm-gear pairs driven by stepper motors. For high angular resolution around the OX and OY axes, the device employs a transmission ratio of 6781 from two motors to these axes. The experimental results reveal that the adjusted average nonparallelism between the measured surface and the surface plate reaches 0.001 mm. The results indicate that the device is fully capable of performing accurate measurements. The device is compact, easy to carry, and low in production cost, making it ideal for installation in small and medium mechanical workshops.

Key words - Angle tilt adjustment; worm-gear; stepper motor; surface plate; accurate measurements

1. Introduction

The foundation of research, design, and development in engineering activities is precise mechanical measurement. It involves assessing various quantities that directly affect the operation and performance of components, devices, or processes. To be valuable, these measurements must be accurate, certain, and reliable [1]. A mechanical detail drawing serves as a comprehensive communication tool between the designer and the manufacturer. It provides clear and concise information about the part's geometry, dimensions, tolerances, materials, and any other necessary details essential for its production and assembly. The dimensional tolerance, shape tolerance, and position tolerance requirements must be carefully reviewed to ensure that the machined part meets the specifications. The 12 geometric characteristic symbols are classified into five categories: form, profile, orientation, location, and runout. [2].

To measure the above geometric characteristics, a datum feature needs to be identified. A datum feature is the actual part surface where a datum symbol on the part drawing references. These datum features are used to establish imaginary axes or planes from which we can measure angles and/or locations. There are several reasons for selecting datum features. In some cases, they are chosen to speed up the manufacturing process of the part. Additionally, datum features can be functional surfaces that help the part seat, mate, and align with other parts during assembly. The primary datum feature, especially if it is a planar surface, should have a large enough surface area to improve the stability of the part during measurement [3].

Two specific examples of measuring flatness and straightness are shown in Figure 1a. To measure the flatness and straightness of the actual surface (1), we first place the bottom surface (3) of part (2) on three levelling screws (6). The magnetic tool holder (7) is placed on the surface plate (5), and the dial indicator tip (8) is brought into contact with the surface to be measured (1). Next, surface (1) is adjusted parallel to surface plate (5) (Figure 1b). Because adjusting two parallel surfaces with levelling screws is time-consuming and requires an experienced technician, there is an urgent need to design a device that simplifies this process. This device eliminates the need for levelling screws altogether.

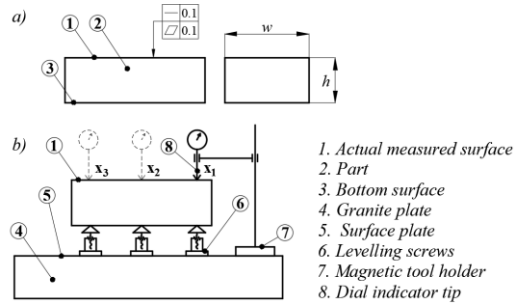

Figure 1. *Example of the preparation process for measuring the straightness and flatness of a surface. a) Straightness and flatness tolerance requirements; b) Adjusting the actual surface parallel to the surface plate*

Large manufacturing companies and measurement and inspection centers often utilize a coordinate measuring machine (CMM) to achieve high accuracy and reduce measurement times. For example, measuring flatness and straightness on CMM involves precisely measuring numerous points on the actual surface and comparing them to a perfect plane. The resulting flatness and straightness errors quantify the surface's deviation of the surface from ideal flatness and straightness, providing valuable insights for quality control and precision manufacturing [4]. However, despite their outstanding advantages, the high cost of CMM machines makes them less feasible for investment by smaller companies or factories.

When CMM measuring machine is not used, to detect the tilt angle around the OX and OY axes, Rajesh et al. proposed the use of two accelerometers. These accelerometers can sense changes in the system's angular position in any direction. The microcontroller then scales the detected change and outputs a corresponding angle tilt value. However, the mechanism for adjusting this angle

measurement was not mentioned in their work [5]. Chen et al. presented a new method using a double ballbar to measure and identify all the geometric errors in a five-axis machine tool tilt table. The method separates errors through a novel fitting technique and verifies identified errors with a comparison between predicted and measured values. The identified errors are used to reduce the ballbar installation errors [6]. In addition, many methods for determining tilt have been proposed, such as techniques for the precise adjustment of the tilt angle of a radio frequency (RF) probe [7], passive radio frequency identification (RFID) technology [8], and the use of a physical model with three sensitive axes of microelectromechanical system (MEMS) accelerometers [9]. After the tilt angle is determined, a mechanical transmission system is set up to adjust that tilt angle. Yuliza et al. described a simple single-axis motion table system for high-resolution tilt sensor testing. The system uses a stepper motor with a resolution of 0.9 degrees per step, which is lower than the requirement of some tilt sensors; a gear system with a 50 transmission ratio was implemented to increase its resolution to 0.018 degrees per step [10]. Shinno et al. designed an X-Y planar motion table system driven by linear motors for high-precision nanomachining applications. The system utilizes eight voice coil motors (VCMs) for precise motion control. VCMs 1 – 4 generate push – pull forces along the X-axis, whereas VCMs 5-8 control the Y-axis through thrust forces. Additionally, by strategically controlling opposing VCMs, the system can achieve minimal Z-axis rotational adjustments to compensate for orientation errors up to 1 μrad [11]. Manual goniometer stages (stages 1-Axis or 2-Axis) manufactured by MISUMI Group Inc. achieve a rotational resolution of 0.1 degrees around the X- and Y-axes. Motorized goniometer stages, on the other hand, achieve a resolution of 0.002 degrees [12]. While Shinno's system achieves exceptional precision through complex control, it also incurs significantly higher manufacturing costs. MISUMI's commercial products also have very high prices.

This study proposes an angle tilt adjustment device, which offers a resolution comparable to that of MISUMI device but at a lower manufacturing cost. On the other hand, by researching, designing, and fabricating the tilt adjustment device itself, the research team gained valuable experience in the technologies needed for developing accurate measurement support devices in the future. Moving forward, the team aims to manufacture the equipment for educational purposes and to make it available for use in measurement tasks via small and medium-sized mechanical workshops.

2. Device design

2.1. Adjusting principle

Figure 2 illustrates how to use three levelling screws to adjust the actual part surface (1) parallel to the surface plate (5) before measuring the flatness and straightness of the surface (1). Three red points p_1, p_2, and p_3, which are located far enough apart on surface (1), are selected, as shown in two ways in Figs. 2b and 2c. The three levelling screws are adjusted so that the three values x_1, x_2, and x_3, obtained from the dial indicator, are equal. At these points, $h_{11} = h_{12} = h_{13}$ indicates that surface (1) is parallel to surface (5).

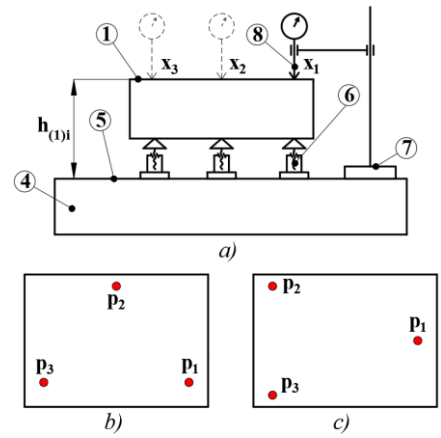

Figure 2. *a) Traditional method for adjusting two-plate parallelism via three-level screws; b) first, 3 points on surfaces (1) are taken from the top view; c) Second, 3 points on surfaces (1) are taken from the top view*

Another approach to adjust the parallelism between the actual surface (1) and the surface plate (5) is to use a mechanism with two trolley-tables that move in independent arcs around the X and Y axes, as shown in Figure 3. The center of rotation of the motion tracks should be symmetrical and perpendicular to the stage surfaces (3 and 5). The principles of parallelism adjustment in this approach are as follows: Part (2) is placed on the surface of the trolley table (3). The dial indicator is used to determine the altitudes of four points p_1, p_2, p_3, and p_4. The values x_1 and x_2 at points p_1 and p_2 are used to determine the angle α_x that trolley-table (3) needs to rotate around the OX axis, whereas the values y_1 and y_2 at points p_3 and p_4 are used to determine the angle α_y that trolley-table (5) needs to rotate around the OY axis.

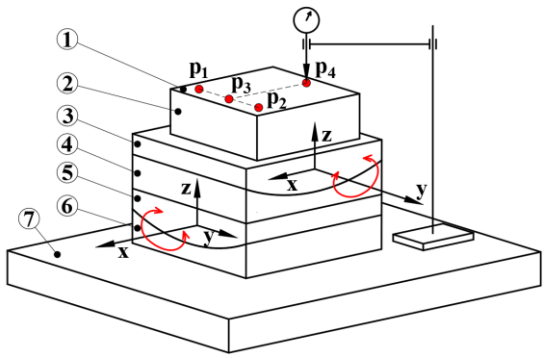

Figure 3. *a) Method for adjusting two-plate parallelism on two trolley tables around the X- and Y-axes; 1. Actual surface; 2. Part; 3. Trolley table 2; 4. Stage 2; 5. Trolley table 1; 6. Stage 1; 7. Surface plate*

The values of the angles α_x and α_y are calculated as follows:

$$\alpha_x = \text{atan}\left[(x_1 - x_2)/l_{p1p2}\right] \quad (1)$$

$$\alpha_y = \text{atan}\left[(y_1 - y_2)/l_{p3p4}\right] \quad (2)$$

where l_{p1p2} and l_{p3p4} are the distances from p_1 to p_2 and p_3 to p_4, respectively. Positive values of α_x and α_y indicate a clockwise rotation direction for trolley-table (3) and trolley-table (5). Conversely, negative values of α_x and α_y correspond to counterclockwise rotation directions of the trolley-table (3) and trolley-table (5), respectively.

2.2. Selecting the motor capacity and transmission ratio

Figure 4 shows the simplified structure of the designed device.

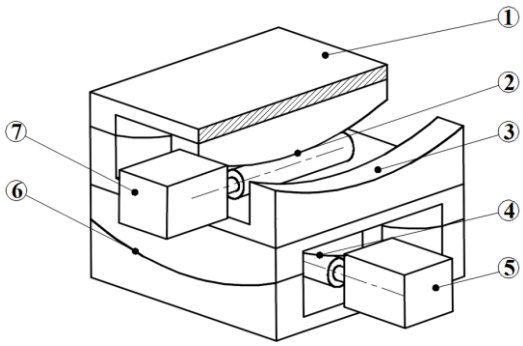

Figure 4. *Device structure; 1. Actual surface; 2 & 4. Worm-gear pairs; 3 & 6. Sliding surface 2; 5&7. Stepper motors X, Y*

Assume that the device is designed to have a load capacity of $m_L = 30$ kg. The relative motion between the trolley-tables and the stages is sliding motion with the sliding friction coefficient taken as $f = 0.3$. Step motor number 5 is chosen to calculate the capacity. Suppose that the total mass of two trolley-tables is $m_{tr} = 2 \times 2.4 = 4.8$ kg, the number of stages is $m_s = 1.15$ kg, the number of worm-gear pairs $m_{w-g} = 0.4$ kg, the number of stepper motors is $m_{sm} = 0.45$ kg. We can calculate the total mass m_T acting on the sliding surface (6) by summing the masses of the components:

$$m_T = m_L + m_{tr} + m_s + m_{w-g} + m_{sm} = 36.8 \text{ kg} \quad (3)$$

The friction force is calculated as follows:

$$F_{ms} = f.N = 0.3 \times 9.81 \times 36.8 = 108.3 \text{ N} \quad (4)$$

The adjustment angle of each trolley-table per second is chosen as $\varphi_{tr} = 0.6^o$. The arc radius of the trolley-tables is chosen to be $r_{tr} = 200$ mm. Therefore, the number of rotations n_{tr}, sliding speed v_s and power N_s of the trolley-table are determined via the following formulas:

$$n_{tr} = \varphi \times \frac{60}{360} = 0.1 \text{ rpm} \quad (5)$$

$$v_s = \varphi_{tr} \times r_{tr} = (0.6\pi/180) \times 0.2 = 0.002 \text{ m/s} \quad (6)$$

$$N_s = F_{ms} \times v_s = 108.3 \times 0.002 = 0.217\ W \quad (7)$$

The efficiencies of the worm-gear pair, the bearing pair, and the coupling are taken as $\eta_{wg} = 0.7$, $\eta_b = 0.95$, $\eta_c = 1$, respectively [13, 14]. Thus, the mechanical transmission system efficiency η_m is calculated as follows:

$$\eta_m = \eta_{wg} \times \eta_b \times \eta_c = 0.665 \quad (8)$$

The power $N_{sh.m}$ on the motor out shaft is determined via the following formula:

$$N_{m.sh} = \frac{N_s}{\eta_m} = 0.326 \text{ W} \quad (9)$$

Because of the small angular resolution needed, the gear ratio of the worm–gear pair is chosen to be $i_{wg} = 500$. The preliminary diameter of the worm wheel is set to $d_{pw} = 500$ mm and the diameter of the screw shaft is set to $d_{ps} = 20$ mm. The following formula is used to calculate the output shaft speed of the motor n_{m-sh} and the torque on the output shaft τ_{m-sh}:

$$n_{m.sh} = n_{tr} \times i_{wg} = 50 \text{ rpm} \quad (10)$$

$$\tau_{m.sh} = 9.55 \times \frac{N_{m-sh}}{n_{m-sh}} = 0.062 \text{ Nm} \quad (11)$$

Based on the requirements for speed and torque on the output shaft, we choose the stepper motor Nema 17, model 17HS19. This motor features a 48mm long body, a 1.68A rated current, an integrated planetary gearbox with a gear ratio $i_{gb} = 13.73$, and a maximum allowed torque of 3 Nm [15]. Thus, the transmission ratio of system i_s and the speed of stepper motor n_{sp} are calculated as follows:

$$i_s = i_{w.g} \times i_{gb} = 6865 \quad (12)$$

$$n_{sp} = n_{m.sh} \times i_{gb} = 686.5 \text{ rpm} \quad (13)$$

2.3. Main material and fabrication parameters

The main parts of the device, including all the materials used in its fabrication process, are detailed in Table 1.

Table 1. *Materials used in the fabrication process*

Part	Material	Part	Material
Trolley tables	AL 6061	Stages	AL 6061
Worm wheel	POM	Worm	C45

The design parameters for the worm wheel and worm are listed in Table 2.

Table 2. *The main worm wheel and worm parameters*

Parameters	Worm wheel	worm
Number of teeth	497	1
Pitch, *mm*	2.5	
Normal module, *mm*	0.8	
Diameter of pitch circle, *mm*	395,5	18,41
Diameter of head circle, *mm*	397	20
Diameter of root circle, *mm*	393,5	16.5

Since the stepper motors have a step angle of 1.8^0, a complete 360^0 rotation requires 200 steps. The minimum rotation angles $\boldsymbol{\alpha_{xmin}}$ and $\boldsymbol{\alpha_{ymin}}$ of the trolley–tables around the OX or OY axes, when the motors complete one step, are calculated as follows:

$$\alpha_{xmin} = \alpha_{ymin} = \frac{1.8^0}{i^*_{wg}.i_{gb}} = \frac{1.8^0}{497 \times 13.73} = 0.00026^0 \quad (14)$$

where i^*_{wg} is the gear ratio of the actual worm–gear pair after adjustment.

2.4. Device control algorithm

The algorithm used to control the proposed device is described in Figure 5. Specifically, the device is placed on the surface plate, and then the measured part is placed on the device's worktable. The foundation of the tool holder is also placed on the surface plate. The digital indicator tip contacts the adjusted actual surface.

Now, the device turns on. The user then proceeds to enter the $L_x = p_1p_2$ and $L_y = p_3p_4$ values. The values of

x_1, x_2, y_1, and y_2 are automatically collected from the digital indicator at points p_1, p_2, p_3, and p_4 (refer to Figure 3). On the basis of these collected values, the tilt angles α_x and α_y are calculated. If x_1 is greater than x_2, this indicates that point p_1 is higher than point p_2. In this case, the X-motor (motor 5 in Figure 4) rotates clockwise by $s_x$steps. Conversely, if x_1 is less than x_2, the X-motor rotates counterclockwise by s_x stpes. If x_1 is equal to x_2, the X-motor remains stationary. A similar comparison is carried out for the y_1 and y_2 values to determine the direction of rotation for the Y-motor (motor 7 in Figure 4). After the angles in X- and Y- axes are adjusted, the adjustment process is finished.

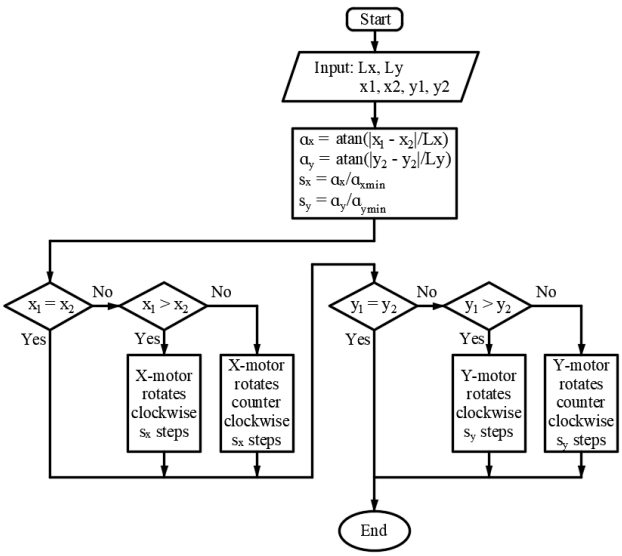

Figure 5. *Flowchart of the device control algorithm*

3. Results and discussion

3.1. 3D model and fabricated device

The 3D model of the device is designed via SolidWorks software, as shown in Figure 6.

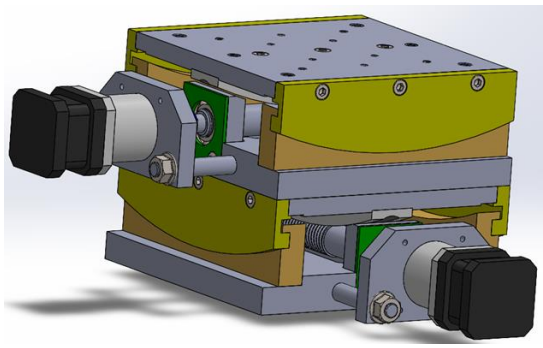

Figure 6. *3D model of the device*

The device has a worktable area of 150x150 mm and a total height of 130 mm. The trolley–tables can rotate a maximum of 30^0, with 15^0 in the clockwise and 15^0 in the counterclockwise direction.

The device is completely fabricated, assembled, and connected to the digital indicator and control system, as shown in Figure 7.

To reduce the time needed to determine the distance between points p_1p_2 and p_3p_4, the working surface is equipped with four reference segments marked in millimeters. Similarly, for easy reference to the X and Y rotation angles of trolley-tables, two reference segments with angular markings (^{o}) are attached to both sides of the device. A digital indicator (Mitutoyo 543-791B-10) with an accuracy of 0.001 mm is connected to the control system for automatic data acquisition. The accuracy of the device depends on many factors, one of the most important being the precision of the mechanical transmission system. Therefore, careful implementation during assembly and alignment is necessary to minimize systematic errors.

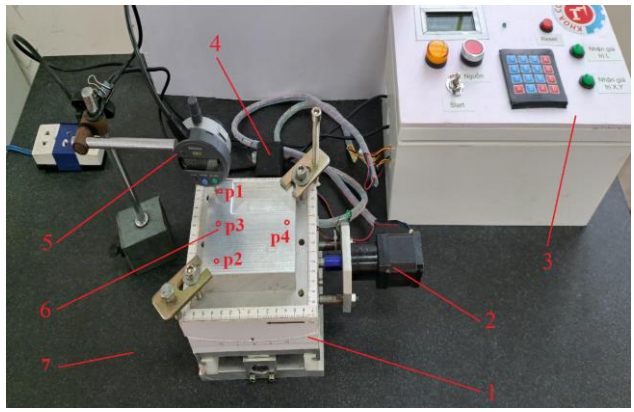

Figure 7. *Real adjusting system; 1. Device; 2. Y-motor; 3. Control system; 4. X-motor; 5. Digital indicator; 6. Actual surface; 7. Surface plate; p1&p2. X-value points; p3&p4. Y-value points*

Figure 8 shows the interface of the device. The sequence for using the interface is as follows: press the "Power" button to supply power to the device; press the "Start" button to start the adjustment process; the 4x4 matrix keyboard is used to input the L_x and L_y values; to confirm the L_x and L_y values, press the "Set values: L_x, L_y" button after entering L_x and L_y in turn; next, move the digital indicator tip to points p_1, p_2, p_3, and p_4, press the "Set values: x_i, y_i" button to confirm the values x_1, x_2, y_1 and y_2, respectively; the controller will then calculate the α_x, α_y, s_x, and s_y values and output the signal to control the X- and Y-motors; the adjustment process is completed; to start a new adjustment process, press the "Reset" button.

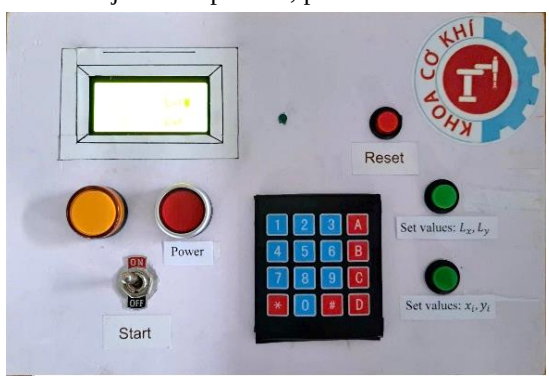

Figure 8. *The device interface*

3.2. Device testing

To test the ability to adjust the tilt angle of the designed device, the x_i and y_i values are repeated 3 times on the same

part that needs to be adjusted, as shown in Figure 7. The standard length tested is $p_1p_2 = p_3p_4 = 80$ mm. Initially, the nonparallelism of the actual surfaces to the surface plate is calculated. These nonparallelism values ($\Delta_{prl.x}$ and $\Delta_{prl.y}$) were calculated via Eqn. 15.

$$\Delta_{prl.x} = |x_1 - x_2|; \Delta_{prl.y} = |y_1 - y_2| \quad (15)$$

After the adjustment process, the nonparallelism between the actual surfaces and the surface plate is calculated again via Eqn. 15. Finally, the average non-parallelism values before and after adjusting are compared, as shown in Table 3.

Table 3. *Nonparallelism before the transmission ratio error is corrected*

	Exp. No	Before adjusting			After adjusting		
		x_1	x_2	$\Delta_{prl.x}$	x_1	x_2	$\Delta_{prl.x}$
Direction X (mm)	#1	-1.488	-2.066	0.578	-1.760	-1.809	0.049
	#2	-1.479	-2.065	0.586	-1.753	-1.803	0.050
	#3	-1.467	-2.058	0.594	-1.749	-1.802	0.053
	Average			0.586	Average		0.051
	Exp. No	y_1	y_2	$\Delta_{prl.y}$	y_1	y_2	$\Delta_{prl.y}$
Direction Y (mm)	#1	-2.079	-1.780	0.299	-1.957	-1.920	0.037
	#2	-2.078	-1.772	0.306	-1.952	-1.914	0.038
	#3	-2.079	-1.769	0.321	-1.947	-1.909	0.038
	Average			0.309	Average		0.038

The average nonparallelism values before and after adjusting are 0.586 and 0.051 in the X direction, and 0.309 and 0.038 in the Y direction, respectively. On the basic of Eqns. 1 and 2, the required α_x and α_y need to be adjusted by 0.4196^0 and 0.2213^0, respectively, to achieve zero nonparallelism in the X and Y directions. Additionally, based on Eqns., however, the real adjusted angles α_x and α_y only reach 0.3832^0 and 0.1941^0, respectively, resulting in differences of 8.67% and 12.29% compared with the required angles. Errors in the system transmission ratio and assembly errors cause this difference. To compensate, offset rotation angles of 8.67% and 12.29% are added in the X and Y directions during adjustment. Following error compensation, the device was retested, and the results presented in Table 4 demonstrate significant improvement.

Table 4. *Nonparallelism after the transmission ratio error is corrected*

	Exp. No	Before adjusting			After adjusting		
		x_1	x_2	$\Delta_{prl.x}$	x_1	x_2	$\Delta_{prl.x}$
Direction X (mm)	#1	-1.471	-2.062	0.591	-1.781	-1.780	0.001
	#2	-1.467	-2.055	0.588	-1.780	-1.780	0.000
	#3	-1.470	-2.063	0.593	-1.785	-1.783	0.002
	Average			0.591	Average		0.001
	Exp. No	y_1	y_2	$\Delta_{prl.y}$	y_1	y_2	$\Delta_{prl.y}$
Direction Y (mm)	#1	-2.075	-1.768	0.307	-1.930	-1.930	0.000
	#2	-2.075	-1.764	0.311	-1.926	-1.928	0.002
	#3	-2.072	-1.759	0.313	-1.922	-1.921	0.001
	Average			0.310	Average		0.001

Table 4 shows an average nonparallelism of 0.001 between the actual surface and the surface plate when adjusted by the proposed system. The device is used to make adjustments on various other machine elements, as shown in Figure 9. The results obtained still show an average nonparallelism within 0.001 mm.

The nonparallelism error is in the range of 0.001 because of the highly sensitive contact measuring tip of the digital indicator, which can be easily affected by dust in the measuring environment. The experimental results demonstrate the proposed device's effectiveness in mechanical measurement applications. However, like any measurement device, the proposed device needs to be periodically calibrated based on the frequency of use to minimize the impact of environmental variables and mechanical wear on data reliability. Currently, the device is checked for accuracy every two weeks.

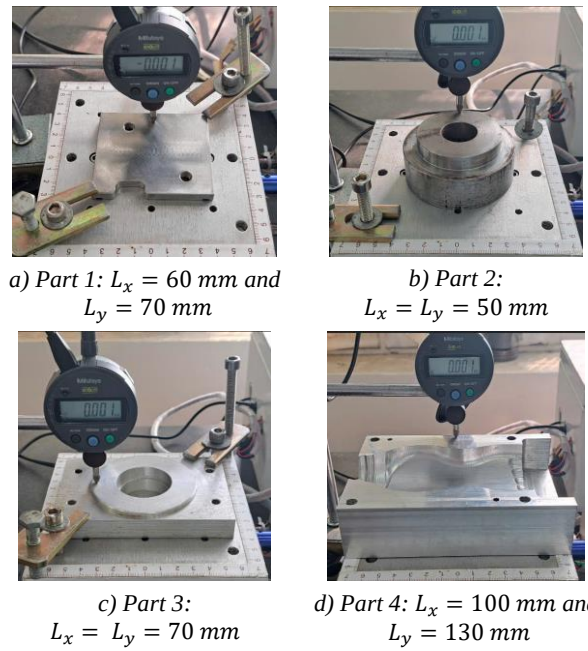

a) Part 1: $L_x = 60$ mm and $L_y = 70$ mm

b) Part 2: $L_x = L_y = 50$ mm

c) Part 3: $L_x = L_y = 70$ mm

d) Part 4: $L_x = 100$ mm and $L_y = 130$ mm

Figure 9. *Adjust the parallelism between the measured surface and the surface plate of some machine elements*

Although CMM machines offer high accuracy and many accompanying features, their cost presents a significant barrier for small-scale companies. Currently, the average price of a CMM machine in the Vietnamese market is over 40,000 USD. The proposed device offers an alternative solution, with a manufacturing cost of under 1,000 USD. Furthermore, in small and medium-sized mechanical workshops, adjusting the measured surface parallel to the surface plate using three leveling screws is both time-consuming and requires skilled technicians. The proposed device significantly reduces adjustment time by 4 to 5 times and minimizes dependence on the technician's skills.

4. Conclusions

This study designed and manufactured a tilt angle adjustment device to make the measured actual surface parallel to a surface plate. The device features two independent stages, each responsible for adjusting the

rotation angle around the OX and OY axes. The proposed device offers a significantly higher resolution of 0.00026 degrees per step of the stepper motor. Additionally, the machine table boasts a generous size of 150 × 150 mm and a load capacity of up to 30 kg, making it suitable for measuring large machine parts. With a very small error of 0.001 mm in the achieved nonparallelism value, the proposed adjustment device is especially useful for precision mechanical measurement applications. Future work should test the replacement of digital indicators with noncontact distance measuring sensors to eliminate errors due to the measurement environment and explore applications of the adjustment device in measuring specific cases of shape and position deviations.

Acknowledgements: This work was supported by The University of Danang - University of Science and Technology, code number of Project: T2023-02-02MSF. The authors thank Tran Ba Phuc and Ha Ngoc Son, students from the 2019 intake of the Faculty of Mechanical Engineering, for their valuable contributions to the device fabrication process.

REFERENCES

[1] T. G. Beckwith, N. L. Buck, and R. D. Marangoni, "*Mechanical measurements"*, Addison-Wesley New York, 1982.

[2] G. R. Cogorno, "*Geometric dimensioning and tolerancing for mechanical design"*, McGraw-Hill Education, 2020.

[3] J. D. Meadows, "*Geometric Dimensioning and Tolerancing: Applications and Techniques for Use in Design: Manufacturing, and Inspection"*, Routledge, 2017.

[4] R. J. Hocken and P. H. Pereira, "*Coordinate measuring machines and systems*", CRC press, 2016.

[5] R. Rajesh and I. Baranilingesan, "Tilt angle detector using 3-axis accelerometer", *International Journal of Scientific Research in Science and Technology*, vol. 4, no. 2, pp. 784-791, 2018, doi: https://doi.org/10.32628/IJSRST1841192.

[6] J. X. Chen, S. W. Lin, X. L. Zhou, and T. Q. Gu, "A ballbar test for measurement and identification the comprehensive error of tilt table", *International Journal of Machine Tools and Manufacture*, vol. 103, pp. 1-12, 2016, doi: https://doi.org/10.1016/j.ijmachtools.2015.12.002.

[7] R. Sakamaki and M. Horibe, "Precision adjustment of probe-tilt angle with RF signal detection technique", *IEEE Transactions on Instrumentation and Measurement*, vol. 69, no. 10, pp. 8500-8505, 2020, doi: https://doi.org/10.1109/TIM.2020.2991601.

[8] X. Lai, Z. Cai, Z. Xie, and H. Zhu, "A novel displacement and tilt detection method using passive UHF RFID technology", *Sensors*, vol. 18, no. 5, p. 1644, 2018, doi: https://doi.org/10.3390/s18051644.

[9] J. Qian, B. Fang, W. Yang, X. Luan, and H. Nan, "Accurate tilt sensing with linear model", *IEEE Sensors Journal*, vol. 11, no. 10, pp. 2301-2309, 2011, doi: https://doi.org/10.1109/JSEN.2011.2121058.

[10] E. Yuliza, H. Habil, R. A. Salam, M. M. Munir, and M. Abdullah, "Development of a Simple Single-Axis Motion Table System for Testing Tilt Sensors", *Procedia Engineering*, vol. 170, pp. 378-383, 2017, doi: https://doi.org/10.1016/j.proeng.2017.03.061.

[11] H. Shinno, H. Yoshioka, and K. Taniguchi, "A newly developed linear motor-driven aerostatic XY planar motion table system for nano-machining", *CIRP Annals*, vol. 56, no. 1, pp. 369-372, 2007, doi: https://doi.org/10.1016/j.cirp.2007.05.086.

[12] MISUMI-Group-Inc., "Motorized Goniometer Stages", *us.misumi-ec.com*, Jun. 29, 2024. [Online]. Available: https://us.misumi-ec.com/vona2/detail/110302633520/. [Accessed

[13] R. L. Mott, "*Machine elements in mechanical design*", Pearson Educación, 2004.

[14] K. Lingaiah, "*Machine Design Data Handbook"*, McGraw-Hill, 1994.

[15] Stepperonline, *"Nema 17 Stepper Motor", omc-stepperonline.com*, Jan. 20, 2023. [Online]. Available: https://www.omc-stepperonline.com/nema-17-stepper-motor-bipolar-l-48mm-w-gear-ratio-14-1-planetary-gearbox-17hs19-1684s-pg14?search=17HS19-1684S-PG14. [Accessed July 07, 2023].